

International Space Station Attitude Control and Energy Storage Experiment: Effects of Flywheel Torque

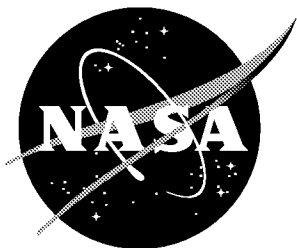
*Carlos M. Roithmayr
Langley Research Center, Hampton, Virginia*

The NASA STI Program Office... in Profile

Since its founding, NASA has been dedicated to the advancement of aeronautics and space science. The NASA Scientific and Technical Information (STI) Program Office plays a key part in helping NASA maintain this important role.

The NASA STI Program Office is operated by Langley Research Center, the lead center for NASA's scientific and technical information. The NASA STI Program Office provides access to the NASA STI Database, the largest collection of aeronautical and space science STI in the world. The Program Office is also NASA's institutional mechanism for disseminating the results of its research and development activities. These results are published by NASA in the NASA STI Report Series, which includes the following report types:

- **TECHNICAL PUBLICATION.** Reports of completed research or a major significant phase of research that present the results of NASA programs and include extensive data or theoretical analysis. Includes compilations of significant scientific and technical data and information deemed to be of continuing reference value. NASA counterpart and peer-reviewed formal professional papers, but having less stringent limitations on manuscript length and extent of graphic presentations.
 - **TECHNICAL MEMORANDUM.** Scientific and technical findings that are preliminary or of specialized interest, e.g., quick release reports, working papers, and bibliographies that contain minimal annotation. Does not contain extensive analysis.
 - **CONTRACTOR REPORT.** Scientific and technical findings by NASA-sponsored contractors and grantees.
 - **CONFERENCE PUBLICATION.** Collected papers from scientific and technical conferences, symposia, seminars, or other meetings sponsored or co-sponsored by NASA.
 - **SPECIAL PUBLICATION.** Scientific, technical, or historical information from NASA programs, projects, and missions, often concerned with subjects having substantial public interest.
 - **TECHNICAL TRANSLATION.** English-language translations of foreign scientific and technical material pertinent to NASA's mission.
- Specialized services that complement the STI Program Office's diverse offerings include creating custom thesauri, building customized databases, organizing and publishing research results... even providing videos.
- For more information about the NASA STI Program Office, see the following:
- Access the NASA STI Program Home Page at ***<http://www.sti.nasa.gov>***
 - E-mail your question via the Internet to help@sti.nasa.gov
 - Fax your question to the NASA STI Help Desk at (301) 621-0134
 - Phone the NASA STI Help Desk at (301) 621-0390
 - Write to:
NASA STI Help Desk
NASA Center for Aerospace Information
7121 Standard Drive
Hanover, MD 21076-1320



International Space Station Attitude Control and Energy Storage Experiment: Effects of Flywheel Torque

*Carlos M. Roithmayr
Langley Research Center, Hampton, Virginia*

National Aeronautics and
Space Administration

Langley Research Center
Hampton, Virginia 23681-2199

February 1999

Available from:

NASA Center for AeroSpace Information (CASI)
7121 Standard Drive
Hanover, MD 21076-1320
(301) 621-0390

National Technical Information Service (NTIS)
5285 Port Royal Road
Springfield, VA 22161-2171
(703) 605-6000

International Space Station Attitude Control and Energy Storage Experiment: Effects of Flywheel Torque

Carlos M. Roithmayr
NASA Langley Research Center, Hampton, Virginia, 23681

November 12, 1998

1 Introduction

Energy storage and attitude control are accomplished with two separate devices on present spacecraft. Batteries are typically used to store and supply electrical energy produced by photovoltaic cells; however, batteries are quite massive, and battery life often limits the life of a spacecraft. Spinning cylinders, such as reaction wheels and control moment gyroscopes, are often employed to control orientation without expending propellant. Although these devices possess a great deal of rotational kinetic energy, there are no provisions to convert it back into electrical form. Mechanical flywheel systems are an attractive alternative to batteries. Their longevity is superior, and they are less massive than batteries; moreover, flywheels can simultaneously store energy and control attitude, making it possible to reduce spacecraft mass even further.

Several advanced technology experiments for the International Space Station (ISS), including the Attitude Control and Energy Storage Experiment (ACESE) led by NASA Lewis Research Center, are currently receiving Phase B funding from the Engineering and Research Technology Program at NASA Johnson Space Center (JSC). ACESE will advance the development of aerospace flywheels by demonstrating the integration of energy storage and attitude control into a single system aboard a working spacecraft.

The experiment consists of two counter-rotating rotors placed in vacuum housings, and levitated with magnetic bearings. Motor-generators will connect the rotors to the existing electrical power system so that they can store energy when it is available from the photovoltaic arrays, and supply energy when it is needed. Each rotor, made up of a metallic hub and a rim of composite material, will be approximately 11 inches in diameter and 13 inches in length, and spin at angular speeds ranging between 15,000 and 50,000 rev/min. ACESE is designed to store the same amount of energy as two batteries; it will be attached to the Station's starboard outboard truss at an unoccupied site for a battery charge-discharge unit and two batteries, and operate in combination with existing batteries. The primary objective of the experiment is to demonstrate energy storage, whereas the secondary objective is to use flywheels to exert torque on the Station, and show

measurable evidence that torque has been applied. In the interest of simplicity, the time history of the magnitude of the torque will be predetermined rather than governed by a feedback control scheme, and the existing Station attitude control system will not be modified to account for presence of the flywheels. The design of ACESE hardware is simplified considerably by omitting devices for measuring directly the torque applied by the experiment to the Station. Measurements can, instead, be obtained indirectly by examining telemetry of CMG torque and momentum. The resolution of CMG momentum measurements is expected to be approximately 100 ft-lb_f-sec, so changes greater than this value can be used to furnish evidence of flywheel torque.

This report presents results of simulations performed to study the behavior of the Station's attitude, and the Control Moment Gyroscopes, when torque is applied by the flywheels in pursuit of the secondary objective, or as a result of a malfunction that occurs while storing or discharging energy. Sec. 2 contains a description of the simulation program and the model of the flywheel system, a derivation of the algorithm for calculating flywheel motor torques, and information regarding mass properties used in the simulations. A discussion of CMG momentum capacity and limits placed on momentum produced by Station equipment appears in Sec. 3 so that it may serve as a basis for evaluating the results associated with the secondary objective, presented in Sec. 4, and the results of simulated malfunctions given in Sec. 5.

2 Simulation Description

The numerical results reported herein were obtained with the Space Station Multi Rigid Body Simulation (SSMRBS; see Ref. [1]), a computer program that numerically integrates equations of motion governing the behavior of a spacecraft modeled as a rigid, multibody, multi-degree-of-freedom system.

SSMRBS is used at JSC by the Aeroscience and Flight Mechanics Division, support contractors, and the Station Guidance, Navigation, and Control (GN&C) prime contractor primarily to evaluate the performance of candidate attitude control schemes for Space Station, and to validate GN&C systems for each stage of the Station assembly sequence. Analysts are able to study the interplay of attitude control with other Space Station activities such as collection of solar power, radiation of excess heat, remote manipulator operations, centrifuge operations, and microgravity experiments. Nominal operations and contingencies are studied, including control of a Station with or without an Orbiter attached, Orbiter docking or separation, and Station reboost.

Simulations typically involve, simultaneously, the control of core body attitude with a control moment gyroscope momentum manager or a reaction control system (or both); independent feedback control of each solar array and radiator joint angle; and transportation of payloads with a mobile transporter or remote manipulator. Analysis involving the ACESE flywheels has been performed at JSC and, more recently, at

the NASA Langley Research Center.

2.1 Model of the Flywheel System

All bodies are treated as rigid in the simulations to be discussed; a flywheel rotor is considered to be a right circular cylinder whose mass is distributed uniformly. The model of the physical connection between a rotor and the outboard truss that is simplest and most appropriate for the study of the Station's attitude behavior is a revolute, or hinge joint whose axis is coincident with the rotor's longitudinal central principal axis of inertia, or spin axis. In such a model of the joint, the spin axis of the rotor is fixed in the outboard truss and in the rotor; that is, the model does not account for any changes in the spin axis direction relative to the outboard truss that are in fact allowed by the magnetic bearings, nor does it permit any coning motions of the rotor. Counter rotation of the two rotors requires that their spin axes be parallel.

Relative motion between a body and its inboard body can be brought about in the simulations by means of a motor; the masses of the two bodies are considered to include the mass of the motor parts. The inboard body exerts torque on the outboard body through the motor, and in accordance with the law of action and reaction, torque of equal magnitude and opposite direction is applied to the inboard body. An ACESE motor-generator is represented by such a motor, whose detailed electrical behavior need not be modeled. The focus of the remainder of this section is the calculation of the torque that must be exerted by each of two motors in order to apply a specified resultant torque to the outboard truss, and change the kinetic energy of the rotor pair at a specified rate.

We begin by denoting the torque exerted by the outboard truss C on rotor A as the vector $\mathbf{T}^{C/A}$, and the torque exerted by C on rotor B as $\mathbf{T}^{C/B}$. The resultant of the two is important in a discussion of the Station's attitude motion, and is given by

$$\mathbf{T}^{C/F} \triangleq \mathbf{T}^{C/A} + \mathbf{T}^{C/B} \quad (1)$$

where F is the system of flywheels formed by rotors A and B .

The rate of change of rotational kinetic energy, or power of the rotors is an important measure of energy storage; thus it is to be specified. The rotational kinetic energy ${}^C K^F$ of F in C is given by

$${}^C K^F = \frac{1}{2} \left({}^C \boldsymbol{\omega}^A \cdot \mathbf{I}^{A/A^*} \cdot {}^C \boldsymbol{\omega}^A + {}^C \boldsymbol{\omega}^B \cdot \mathbf{I}^{B/B^*} \cdot {}^C \boldsymbol{\omega}^B \right) \quad (2)$$

where ${}^C\boldsymbol{\omega}^A$ and ${}^C\boldsymbol{\omega}^B$ are, respectively, the angular velocities of A and B in (or relative to) C , and where $\underline{\mathbf{I}}^{A/A^*}$ and $\underline{\mathbf{I}}^{B/B^*}$ are the inertia dyadics of A and B relative to their respective mass centers, A^* and B^* . The power ${}^CP^F$ of F in C is defined as the derivative of ${}^CK^F$ with respect to time, therefore

$$\begin{aligned} {}^CP^F &\triangleq \frac{d}{dt} {}^CK^F \\ &= \frac{1}{2} \left(\frac{d}{dt} {}^C\boldsymbol{\omega}^A \cdot \underline{\mathbf{I}}^{A/A^*} \cdot {}^C\boldsymbol{\omega}^A + {}^C\boldsymbol{\omega}^A \cdot \frac{d}{dt} \underline{\mathbf{I}}^{A/A^*} \cdot {}^C\boldsymbol{\omega}^A + {}^C\boldsymbol{\omega}^A \cdot \underline{\mathbf{I}}^{A/A^*} \cdot \frac{d}{dt} {}^C\boldsymbol{\omega}^A + \right. \\ &\quad \left. \frac{d}{dt} {}^C\boldsymbol{\omega}^B \cdot \underline{\mathbf{I}}^{B/B^*} \cdot {}^C\boldsymbol{\omega}^B + {}^C\boldsymbol{\omega}^B \cdot \frac{d}{dt} \underline{\mathbf{I}}^{B/B^*} \cdot {}^C\boldsymbol{\omega}^B + {}^C\boldsymbol{\omega}^B \cdot \underline{\mathbf{I}}^{B/B^*} \cdot \frac{d}{dt} {}^C\boldsymbol{\omega}^B \right) \end{aligned} \quad (3)$$

where all vectors and dyadics are differentiated with respect to time in the same reference frame C , as indicated with the notation ${}^Cd/dt$. One may recognize, first, that $\underline{\mathbf{I}}^{A/A^*}$ and $\underline{\mathbf{I}}^{B/B^*}$ do not change with time in C because the joints connecting A and B to C are parallel to the axes of symmetry of the rotors, and second, that the angular accelerations ${}^C\boldsymbol{\alpha}^A$ and ${}^C\boldsymbol{\alpha}^B$ of A and B in C are defined respectively by

$${}^C\boldsymbol{\alpha}^A \triangleq \frac{d}{dt} {}^C\boldsymbol{\omega}^A, \quad {}^C\boldsymbol{\alpha}^B \triangleq \frac{d}{dt} {}^C\boldsymbol{\omega}^B \quad (4)$$

Hence, ${}^CP^F$ can be expressed as

$${}^CP^F = \left(\underline{\mathbf{I}}^{A/A^*} \cdot {}^C\boldsymbol{\alpha}^A \right) \cdot {}^C\boldsymbol{\omega}^A + \left(\underline{\mathbf{I}}^{B/B^*} \cdot {}^C\boldsymbol{\alpha}^B \right) \cdot {}^C\boldsymbol{\omega}^B \quad (5)$$

By appealing to the angular momentum principle, and assuming that the moment of all forces exerted on a rotor about the rotor's mass center is equal to the torque exerted by C on the rotor, we may write

$$\mathbf{T}^{C/A} = \underline{\mathbf{I}}^{A/A^*} \cdot {}^C\boldsymbol{\alpha}^A + {}^C\boldsymbol{\omega}^A \times \underline{\mathbf{I}}^{A/A^*} \cdot {}^C\boldsymbol{\omega}^A, \quad \mathbf{T}^{C/B} = \underline{\mathbf{I}}^{B/B^*} \cdot {}^C\boldsymbol{\alpha}^B + {}^C\boldsymbol{\omega}^B \times \underline{\mathbf{I}}^{B/B^*} \cdot {}^C\boldsymbol{\omega}^B \quad (6)$$

Now, the revolute joint ensures that the angular velocity ${}^C\boldsymbol{\omega}^A$ is always parallel to a central principal axis of inertia of A ; therefore, the term ${}^C\boldsymbol{\omega}^A \times \underline{\mathbf{I}}^{A/A^*} \cdot {}^C\boldsymbol{\omega}^A$ vanishes. Likewise, the counterpart of this term for rotor B also vanishes. We thus obtain

$$\mathbf{T}^{C/A} = \underline{\mathbf{I}}^{A/A^*} \cdot {}^C\boldsymbol{\alpha}^A, \quad \mathbf{T}^{C/B} = \underline{\mathbf{I}}^{B/B^*} \cdot {}^C\boldsymbol{\alpha}^B \quad (7)$$

Substitution from Eqs. (7) and (1) into (5) yields

$$\begin{aligned} {}^CP^F &= \mathbf{T}^{C/A} \cdot {}^C\boldsymbol{\omega}^A + \mathbf{T}^{C/B} \cdot {}^C\boldsymbol{\omega}^B \\ &= \left(\mathbf{T}^{C/F} - \mathbf{T}^{C/B} \right) \cdot {}^C\boldsymbol{\omega}^A + \mathbf{T}^{C/B} \cdot {}^C\boldsymbol{\omega}^B \\ &= \mathbf{T}^{C/F} \cdot {}^C\boldsymbol{\omega}^A + \mathbf{T}^{C/B} \cdot ({}^C\boldsymbol{\omega}^B - {}^C\boldsymbol{\omega}^A) \end{aligned} \quad (8)$$

In order to proceed to express the right hand member in terms of scalars, it is convenient to introduce a unit vector $\hat{\boldsymbol{\lambda}}$ parallel to the rotor spin axes, fixed in rotors A and B , and in the outboard truss C . We then define the following three scalars

$$T^{C/A} \triangleq \mathbf{T}^{C/A} \cdot \hat{\boldsymbol{\lambda}}, \quad T^{C/B} \triangleq \mathbf{T}^{C/B} \cdot \hat{\boldsymbol{\lambda}}, \quad T^{C/F} \triangleq \mathbf{T}^{C/F} \cdot \hat{\boldsymbol{\lambda}} \quad (9)$$

and write the angular velocities of A and B in C as

$${}^C\boldsymbol{\omega}^A \triangleq u_A \hat{\boldsymbol{\lambda}}, \quad {}^C\boldsymbol{\omega}^B \triangleq u_B \hat{\boldsymbol{\lambda}} \quad (10)$$

where u_A and u_B are angular speeds in C of A and B , respectively. After substituting from Eqns. (9) and (10) into (8), forming the indicated scalar products, and solving the resulting expression for $T^{C/B}$, one obtains

$$T^{C/B} = \frac{{}^C P^F - T^{C/F} u_A}{u_B - u_A} \quad (11)$$

In addition, the scalar product of Eq. (1) with $\hat{\boldsymbol{\lambda}}$ yields, after rearrangement,

$$T^{C/A} = T^{C/F} - T^{C/B} \quad (12)$$

With the ${}^C P^F$ and $T^{C/F}$ specified, and the rotor angular speeds u_A and u_B known, Eqs. (11) and (12) are used¹, in order, to calculate the $\hat{\boldsymbol{\lambda}}$ -measure numbers of the torques to be applied by motors to B and A . With ${}^C P^F > 0$, the flywheels are charging; that is, rotational kinetic energy in C of F is increasing. Torque is applied by F to C in the direction of $\hat{\boldsymbol{\lambda}}$ when $T^{C/F} < 0$.

When ACESE is to be used solely to store and supply energy, without exerting torque on the Station, $T^{C/F}$ is set to zero. In addition, the angular speeds of the rotors should begin with identical values and opposite signs; that is, $u_A = -u_B$. In view of Eq. (11), $T^{C/B} = {}^C P^F / (2u_B)$, and, in view of Eq. (12), $T^{C/A} = -T^{C/B}$. Under these conditions, the absolute values of u_A and u_B will remain identical.

2.2 Mass Distribution of Station Bodies, Rotors

The Space Station is modeled as a collection of 15 rigid bodies fastened together: a core body, outboard truss structures, solar arrays, radiators, and so forth. The mass distribution for each body, and the topography of the spacecraft are as described for configuration c080_13a in Ref. [2]. Two additional bodies attached to the starboard outboard truss represent the flywheel rotors. The masses of A and B are given by $m_A = m_B = 2.17$ slugs, and the central inertia dyadics are given by $\underline{\mathbf{I}}^{A/A^*} = \underline{\mathbf{I}}^{B/B^*} = 0.294 \hat{\mathbf{c}}_1 \hat{\mathbf{c}}_1 + 0.222 \hat{\boldsymbol{\lambda}} \hat{\boldsymbol{\lambda}} + 0.294 \hat{\mathbf{c}}_3 \hat{\mathbf{c}}_3$ slug-ft², where $\hat{\mathbf{c}}_1$ and $\hat{\mathbf{c}}_3$ are any two unit vectors perpendicular to each other and to $\hat{\boldsymbol{\lambda}}$.

3 CMG Momentum Capacity, Payload Momentum Limits

Evaluation of the following simulation results is facilitated by knowing the angular momentum capacity of the Station's Control Moment Gyroscopes (CMGs), and limits placed upon angular momentum that can be produced by payloads or experiments during the time that microgravity experiments are being conducted.

¹Eqns. (11) and (12) are in agreement with Eqs. (7) and (8) in notes provided by Michael Oshima at Boeing (Seattle) on Sept. 2, 1997.

The magnitude of central angular momentum in an inertial reference frame that each CMG can possess is limited to 3500 ft-lb_f-sec; when all four CMGs are operating, the magnitude of the resultant of the angular momenta can reach 14000 ft-lb_f-sec. However, the Station's reaction control system jets will expend propellant (and disturb any microgravity experiments in progress) to desaturate the CMGs if their momentum reaches 13000 ft-lb_f-sec. In comparison, one flywheel rotor possesses approximately 1160 ft-lb_f-sec of angular momentum at high speed ($0.222 \text{ slug-ft}^2 \times 50000 \text{ rev/min}$); that is, about $\frac{1}{3}$ of the momentum of a CMG. It is useful to keep this in mind when reading Secs. 4 and 5.

During nominal operations aboard the Assembly Complete configuration, equipment on the United States On-orbit Segment (which includes the outboard truss structures) is not permitted to impart more than 1600 ft-lb_f-sec (see Ref. [3]) to the Station while microgravity experiments are being conducted. Although this limit is not strictly applicable to the 13a configuration, or to contingencies, it nevertheless furnishes a useful measure for assessing the results reported in Sec. 5.

4 Flywheel Torque Assist for CMGs

The goal of using ACESE to exert torque on the Station, and demonstrate measurable evidence thereof, gives rise to questions of the direction and magnitude of the torque that will be best for this purpose. In terms of the symbols already introduced, we wish to know how should $\hat{\lambda}$ be oriented in C , and what mathematical form should $T^{C/F}$ take.

As it turns out, the orientation of the rotor spin axes in C is dictated more by the geometry of the ACESE enclosure and the site to which it is to be attached, than by considerations of the secondary goal. However, it is fortuitous that the geometrical constraints lead to a direction of $\hat{\lambda}$ that facilitates attitude control. The rotors are packaged most easily with $\hat{\lambda}$ in the same direction as \hat{c}_2 , a unit vector fixed in the outboard truss and parallel to the axis of the revolute joint (known as the alpha joint) that connects the outboard truss to the Station core body. Unit vector \hat{c}_2 is thus fixed also in the core body, in what is called the Station "y" direction, leading to analytical and operational simplifications regarding the direction of the torque applied by rotors A and B to the Station.

A sinusoidal form for $T^{C/F}$ is suggested by two aspects of the flywheel experiment. First, as the Station passes from sunlight into the Earth's shadow, and back into sunlight, the flywheels will alternately charge with electricity from the solar arrays, and discharge their energy into the power system. Second, exerting torque with the flywheel pair will require their spin speeds to become unequal, and this process must eventually be reversed so that the flywheel pair will again be in a position to store energy without exerting torque on the Station.

If possible, torque should be applied by the flywheels in such a way as to assist the CMGs in their job of

controlling the orientation of the Station core body, keeping it in “torque equilibrium attitude”. Although it may be possible to obtain measurable evidence of applied torque with an arbitrary time history of $T^{C/F}$, it makes more sense to anticipate the torque to be exerted by the CMGs on the core body, and attempt to supply part of this with the flywheels. Simulation results for Station configuration 13A, with $T^{C/A} = T^{C/B} = 0$, are shown in Fig. 1 for a time interval during which attitude motion has reached steady-state; the torque exerted by the CMGs on the core body is projected into unit vectors $\hat{\mathbf{b}}_1$, $\hat{\mathbf{b}}_2$, and $\hat{\mathbf{b}}_3$ fixed in the core body and parallel to the Station “x”, “y”, and “z” directions respectively. The alpha joint that attaches the core body to the outboard truss keeps $\hat{\mathbf{b}}_2$ equal to $\hat{\mathbf{c}}_2$ (and therefore to $\hat{\boldsymbol{\lambda}}$) at all times. Inspection of Fig. 1 reveals that the $\hat{\mathbf{b}}_2$ measure number of CMG torque is nearly a simple sinusoid, whereas the other two curves can not be represented well with this simple mathematical form. The orbital period of the Station is in this case approximately 5560 sec, so the sinusoid has a frequency of two cycles per orbit.

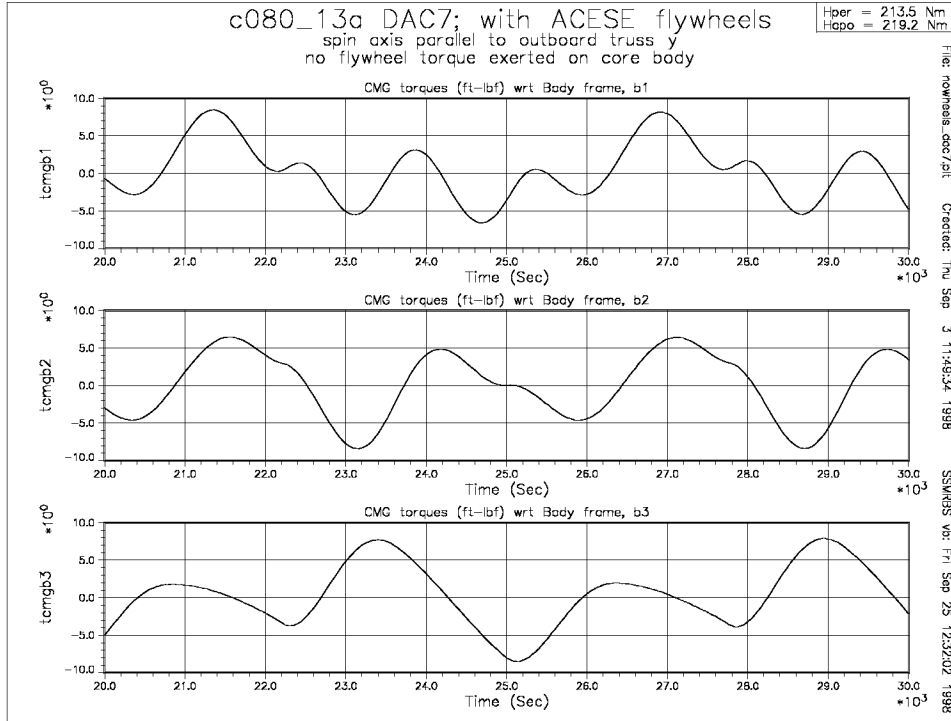


Figure 1: CMG Torque, No Flywheel Motion

Consequently, the form chosen for $T^{C/F}$ is

$$T^{C/F} = \tau \sin 2\omega(t - t^*) \quad (13)$$

where ω is the frequency at which the Station orbits the Earth, and t^* is a particular value of the time t at which the $\hat{\mathbf{b}}_2$ measure number of CMG torque is zero, and has a positive slope. The angular speeds u_A and u_B of the rotors should remain, approximately, less than 50,000 rev/min, and greater than 15,000 rev/min; this requirement, together with the value of the axial central principal moment of inertia of the

rotors, effectively limits the absolute value of τ to 0.75 ft-lb_f (1.017 N-m). The second plot from Fig. 1 is redisplayed in Fig. 2 with a solid curve, and a plot of $T^{F/C} \triangleq -T^{C/F}$ is displayed with a dashed curve, where $T^{C/F}$ is given by Eq. (13) with $\tau = -0.75$ ft-lb_f, $\omega = 0.0011295$ rad/sec, and $t^* = 20860$ sec. Prior to $t = t^*$, $\tau = 0$.

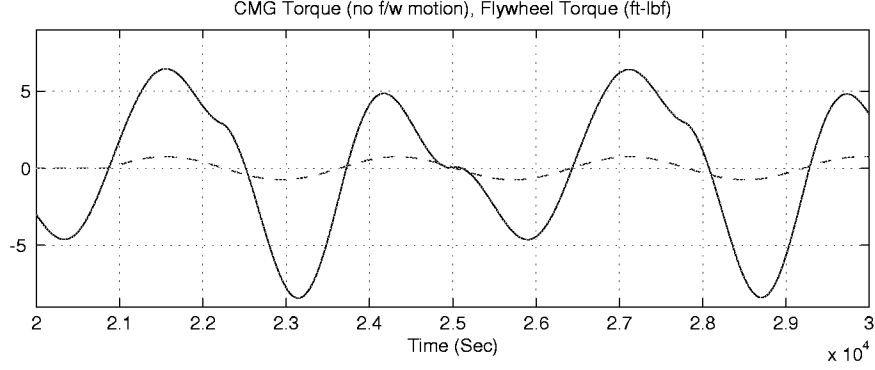


Figure 2: CMG Torque, Flywheel Torque ($T^{F/C}$)

A simulation of using the flywheels for simultaneous assistance of the CMGs and energy storage is performed, where $T^{C/B}$ and $T^{C/A}$ are calculated according to Eqs. (11) and (12) for $t \geq t^*$. ${}^C P^F$ is specified as 2200 watts during the sunlit portion of an orbit, and as -1.57×2200 watts during eclipse. (In these particular simulations, the ratio of time spent by the spacecraft in sunlight to that spent in eclipse is 1.57.) $T^{F/C}$ is specified as indicated in Fig. 2. The results are exhibited with a solid curve in the upper plots of Figs. (3)–(5), and compared to results of the simulation in which flywheel torque is absent ($T^{C/A} = T^{C/B} = 0$), shown with a broken curve. The lower plot shows the difference between the two curves in the upper plot; specifically, the values displayed with the solid curve (flywheel torque present) are subtracted from the values displayed with the broken curve (flywheel torque absent).

The reduction in the $\hat{\mathbf{b}}_2$ measure number of torque exerted by the CMGs as a consequence of assistance from the flywheels is illustrated in Fig. (3) over the interval $30000 \text{ sec} \leq t \leq 40000 \text{ sec}$. The decrease, quantified in the lower plot, is seen to have the form of Eq. (13), with an amplitude of very nearly 0.75 ft-lb_f.

The reduction in CMG torque is reflected in a smaller magnitude of the resultant of central angular momenta in inertial space of the four CMGs, as shown in Fig. 4. The difference is displayed in the lower plot; a positive value in this case indicates a reduction in momentum magnitude, which periodically reaches 200 ft-lb_f-sec.

The CMG momentum management scheme used in these simulations places greater emphasis on controlling orientation than on minimizing CMG momentum; therefore, one expects to see only small differences in the roll, pitch, and yaw of the core body with respect to, say, a local-vertical-local-horizontal reference frame. Such expectations are in fact borne out; of the three orientation angles, the largest difference occurs

in pitch and is less than 0.18 deg, and is transient in nature as shown in Fig. 5.

The foregoing differences in CMG torque and momentum should be in evidence in telemetry transmitted from the Station, providing measurable confirmation of the sinusoidal torque exerted by the flywheels. Differences in core body attitude are less likely to furnish a clear demonstration of the experiment's success.

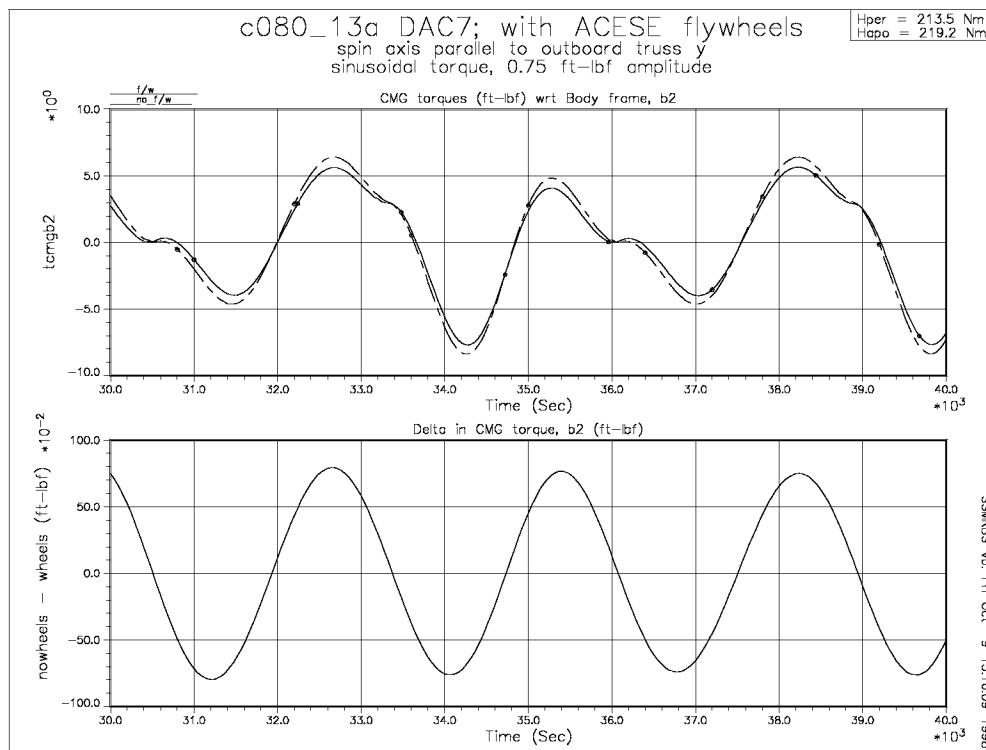


Figure 3: CMG Torque, with and without Flywheels

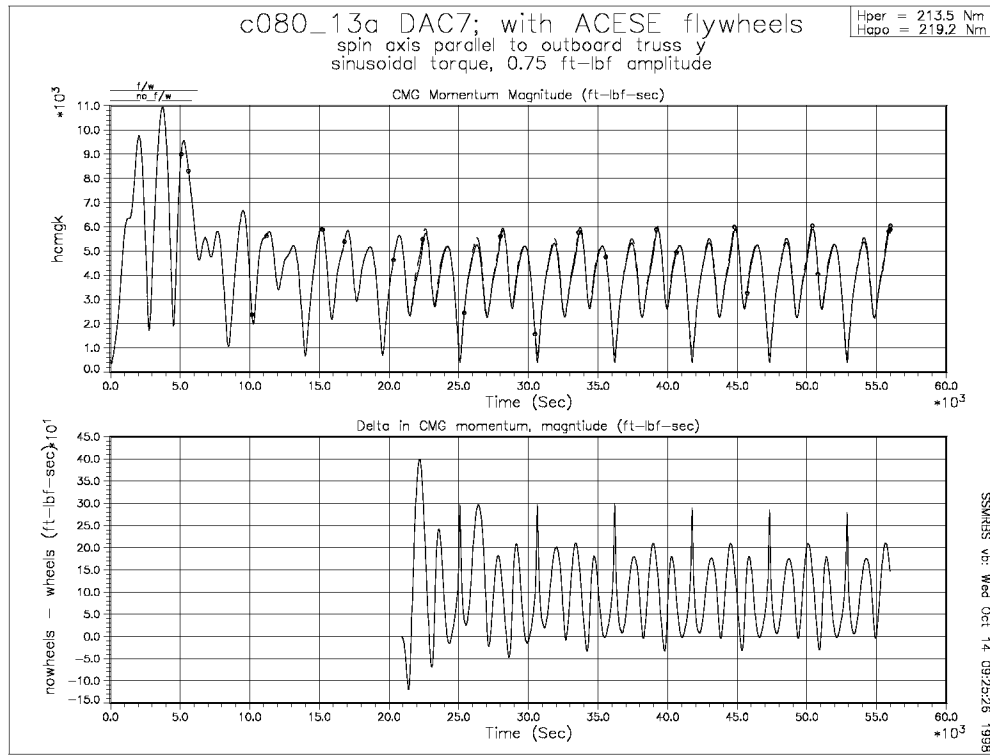


Figure 4: CMG Angular Momentum Magnitude

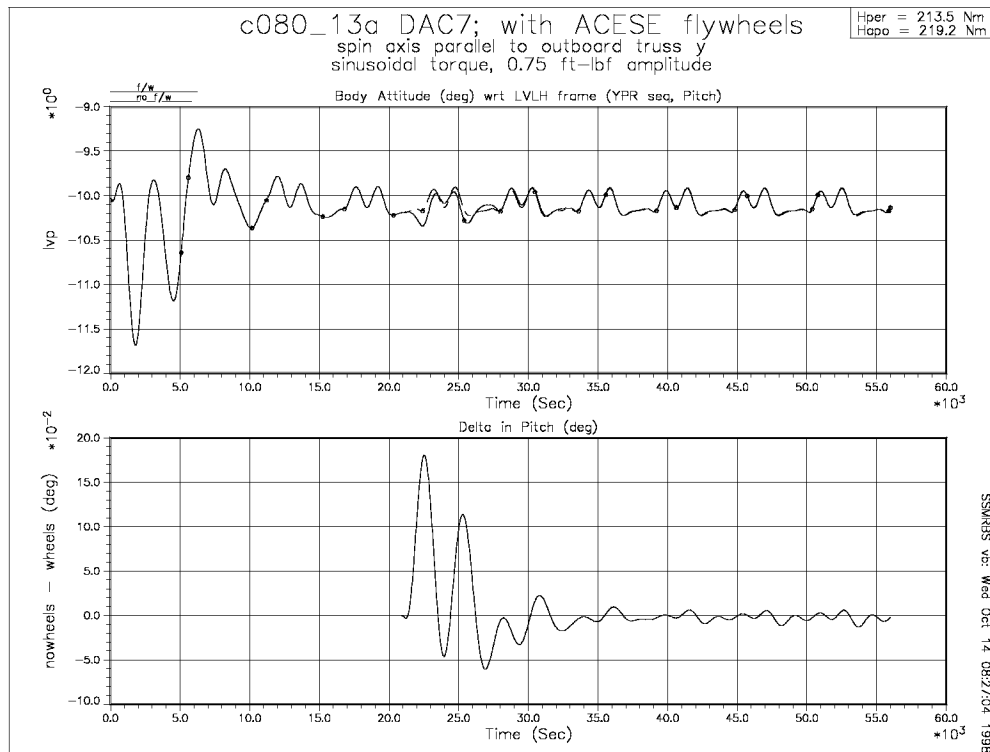


Figure 5: Core Body Pitch Relative to LVLH

5 Energy Storage Contingencies

Ideally, the storage and discharge of energy takes place as the rotors are counter rotating (${}^C\boldsymbol{\omega}^A = -{}^C\boldsymbol{\omega}^B$), and no torque is applied by the flywheel pair to the outboard truss C . However, malfunctions can occur in which the rotors no longer counter rotate, and $T^{F/C}$ differs from 0. One such situation involves having to bring a rotor to an abrupt stop while the other rotor continues to spin. A second condition of this kind occurs when energy storage must be performed with one rotor because it is not possible to operate the second rotor. Both of these situations are examined in what follows.

5.1 Emergency Shutdown of One Rotor

An abrupt stop of one rotor is simulated by starting with initial values $u_B(t=0) = -u_A(t=0) = 50000$ rev/min, setting $T^{C/A} = T^{C/B} = 0$ for $0 \leq t < 20860$ sec, and then making $T^{C/B} = -2$ ft-lb_f for $20860 \leq t \leq 21441$ sec. In this way B is brought to rest in C , while the angular speed u_A remains equal to -50000 rev/min. As in the previous section, results are compared to those of the simulation in which $T^{C/A} = T^{C/B} = 0$ at all times, and $u_A(t=0) = u_B(t=0) = 0$. Several parameters are examined, and the greatest differences observed in each are reported in Table 1. “Attitude, wrt LVLH” refers to the orientation of the Station core body relative to a local-vertical-local-horizontal reference frame, described with a body-three, 3-2-1 (yaw, pitch, roll) rotation sequence. The $\hat{\mathbf{b}}_1$ - $\hat{\mathbf{b}}_2$ - $\hat{\mathbf{b}}_3$ measure numbers of the resultant of the four CMG central angular momenta, and the resultant CMG torque, are examined. In addition, the magnitude of the CMG momentum is shown in the final column. Time histories of two parameters are shown: Fig. 6 displays the core body pitch angle, and Fig. 7 shows the $\hat{\mathbf{b}}_2$ -measure number of CMG momentum. The differences in attitude and CMG torque are not significant, and the difference in CMG momentum magnitude is within the limits set for payload angular momentum during microgravity operations aboard Assembly Complete (see Sec. 3).

Table 1: Effects of Rotor Shutdown

	yaw	pitch	roll	
Attitude, wrt LVLH (deg)	0.023	0.350	0.035	
	$\cdot \hat{\mathbf{b}}_1$	$\cdot \hat{\mathbf{b}}_2$	$\cdot \hat{\mathbf{b}}_3$	magnitude
CMG Angular Momentum (ft-lb _f -sec)	75	1600	100	850
CMG Torque (ft-lb _f)	0.12	3.3	0.19	–

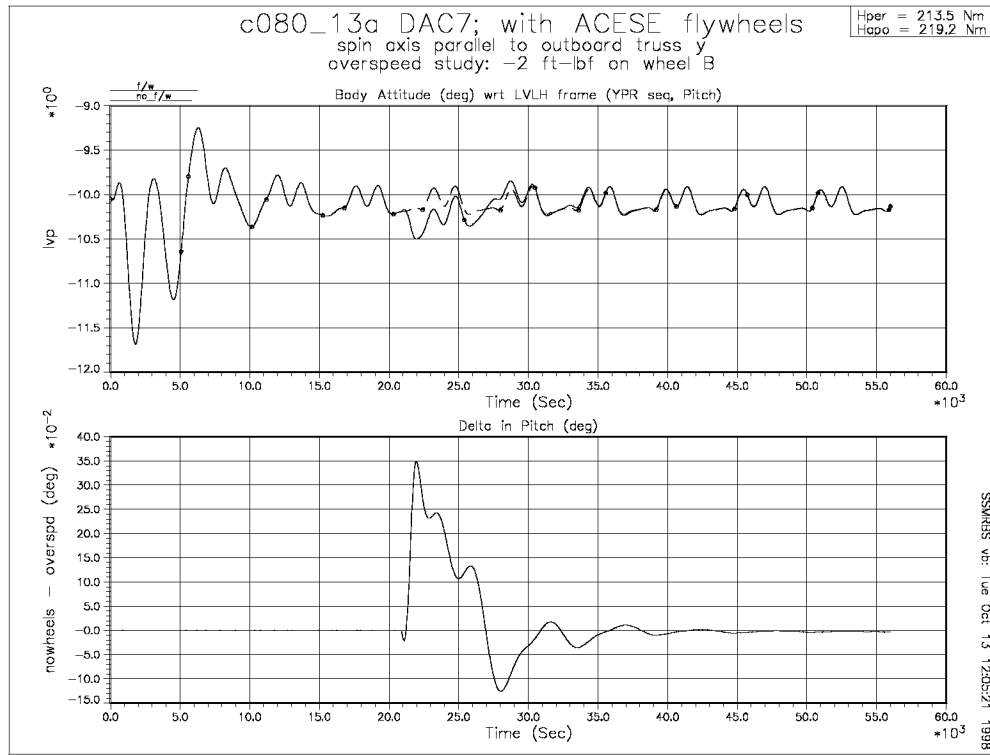


Figure 6: Core Body Pitch Relative to LVLH

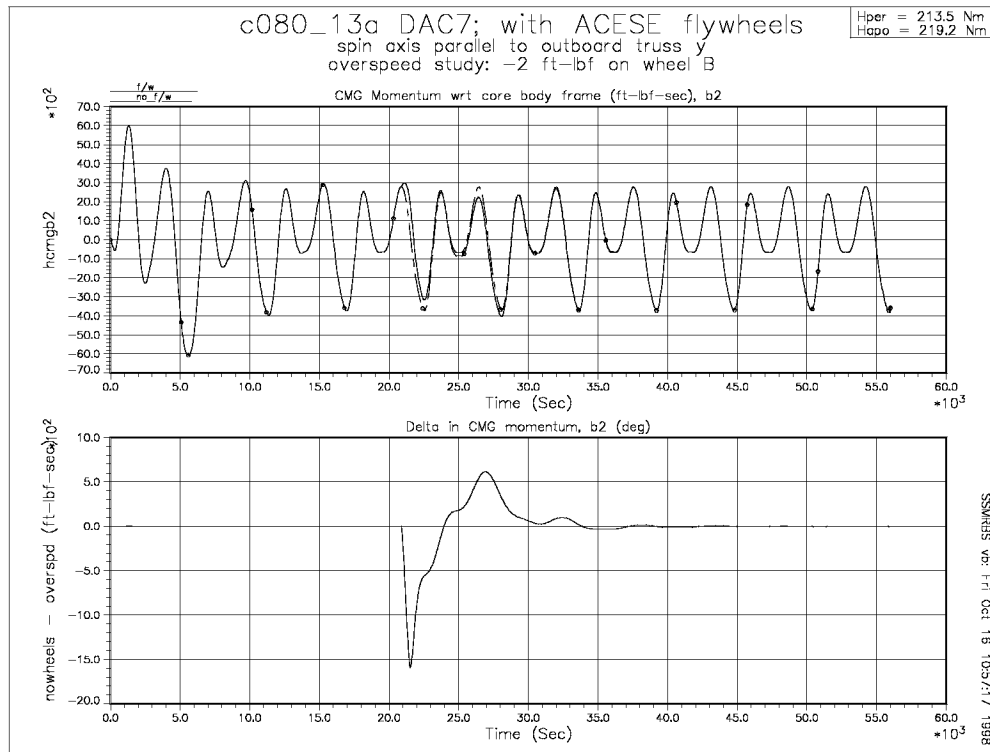


Figure 7: \hat{b}_2 measure number of CMG momentum

5.2 Energy Storage Using a Single Rotor

Should one rotor become incapacitated, it may be possible to demonstrate energy storage at a reduced level with the remaining rotor. Supposing that A is regarded as the malfunctioning rotor, the event is simulated by setting $T^{C/F}$ to 0 in Eq. (11), and by specifying ${}^C P^F$ as 1100 watts when the spacecraft receives sunlight, and -1.57×1100 watts when the spacecraft is in darkness. Instead of calculating $T^{C/A}$ according to Eq. (12), it is defined to be 0 throughout the simulation.

The particular initial values of orbit parameters and position of the sun in these simulations make it convenient to choose $u_B(t = 0) = 38000$ rev/min; thereafter, u_B varies between 51000 and 19000 rev/min. Since A is to be at rest in C , u_A is chosen as 0 at $t = 0$, and remains exceedingly small for the duration of the simulation.

As before, results are compared to those of the simulation in which $T^{C/A} = T^{C/B} = 0$ at all times, and the greatest differences observed are reported in Table 2. Time histories of core body pitch and the $\hat{\mathbf{b}}_2$ -measure number of CMG momentum are shown in Figs. 8 and 9 respectively. The differences seen in attitude and CMG torque are not significant, and the difference in CMG momentum magnitude is within the limits set for payload angular momentum during microgravity operations aboard Assembly Complete (see Sec. 3).

Table 2: Effects of Single-Rotor Energy Storage

	yaw	pitch	roll	
Attitude, wrt LVLH (deg)	0.010	0.140	0.019	
	$\cdot \hat{\mathbf{b}}_1$	$\cdot \hat{\mathbf{b}}_2$	$\cdot \hat{\mathbf{b}}_3$	magnitude
CMG Angular Momentum (ft-lb _f -sec)	55	650	100	300
CMG Torque (ft-lb _f)	0.12	1.2	0.12	—

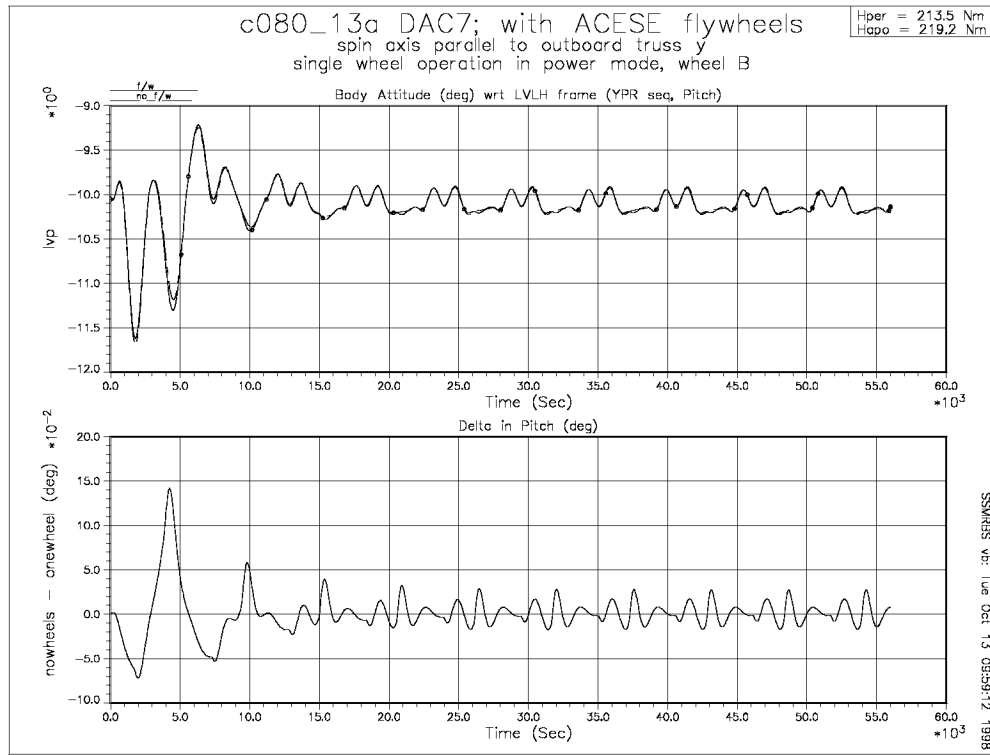


Figure 8: Core Body Pitch Relative to LVLH

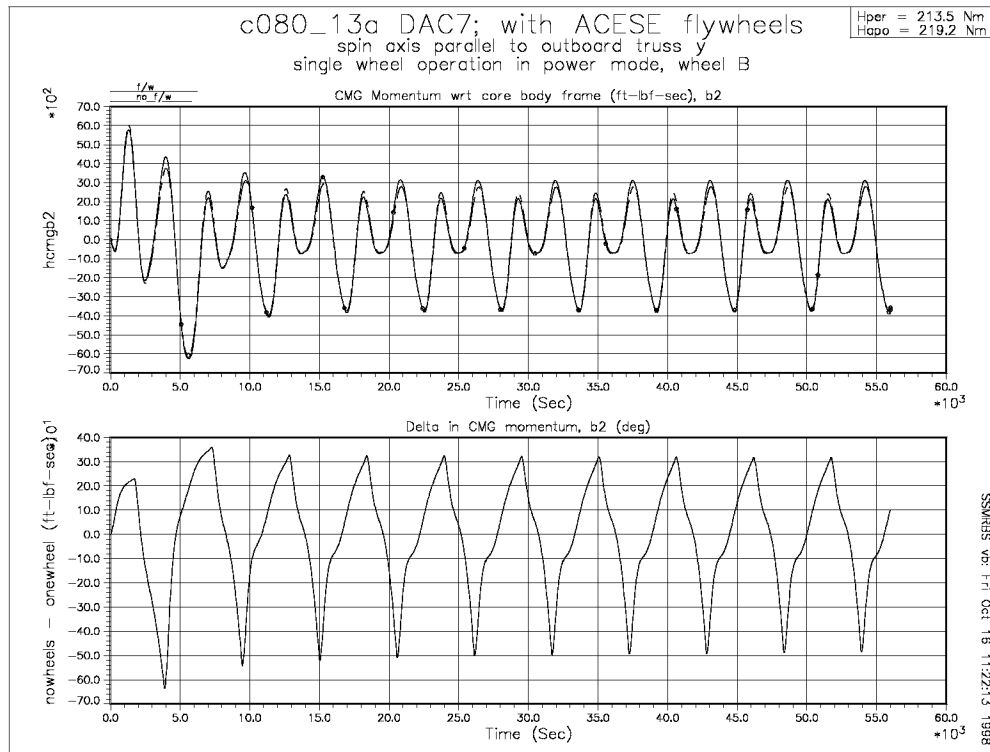


Figure 9: \hat{b}_2 measure number of CMG momentum

6 Conclusions

The secondary objective of the ACESE experiment, to contribute torque for Station attitude control while storing or discharging energy, can be achieved by matching the phase of the sinusoidal torque exerted by CMGs when attitude motion reaches steady state. Although the amplitude of the torque exerted by the flywheels is much less than that of the CMGs, a reduction in CMG torque and momentum should be evident in telemetry of those parameters.

Two ACESE contingencies were studied: the abrupt stop of one rotor while the other rotor continues to spin at high speed, and energy storage with one rotor instead of a counter rotating pair. In each case, Station attitude and CMG torque were not affected significantly, and CMG momentum remains within limits established for microgravity operations aboard the Assembly Complete station configuration.

References

- [1] "Space Station Multi Rigid Body Simulation User's Guide", version b2.0, TM-DYNACS-98-HM28, prepared for NASA Johnson Space Center by Dynacs Engineering Co. Inc., Houston, TX, October 26, 1998.
- [2] "International Space Station On-Orbit Assembly, Modeling, and Mass Properties Databook; Design Analysis Cycle #7, Revision D Assembly Sequence", JSC-26557, Rev. I, Vol. 1, NASA Johnson Space Center, Houston, TX, September, 1998.
- [3] "System Specification for the International Space Station, Advanced Copy", SSP 41000H, prepared for NASA by Boeing Defense and Space Group, Missiles and Space Division, Houston, Tx, May 25, 1998, p. 39.

REPORT DOCUMENTATION PAGE			Form Approved OMB No. 0704-0188	
Public reporting burden for this collection of information is estimated to average 1 hour per response, including the time for reviewing instructions, searching existing data sources, gathering and maintaining the data needed, and completing and reviewing the collection of information. Send comments regarding this burden estimate or any other aspect of this collection of information, including suggestions for reducing this burden, to Washington Headquarters Services, Directorate for Information Operations and Reports, 1215 Jefferson Davis Highway, Suite 1204, Arlington, VA 22202-4302, and to the Office of Management and Budget, Paperwork Reduction Project (0704-0188), Washington, DC 20503.				
1. AGENCY USE ONLY (Leave blank)		2. REPORT DATE February 1999	3. REPORT TYPE AND DATES COVERED Technical Memorandum	
4. TITLE AND SUBTITLE International Space Station Attitude Control and Energy Storage Experiment: Effects of Flywheel Torque			5. FUNDING NUMBERS 906-430-00-01	
6. AUTHOR(S) Carlos M. Roithmayr				
7. PERFORMING ORGANIZATION NAME(S) AND ADDRESS(ES) NASA Langley Research Center Hampton, VA 23681-2199			8. PERFORMING ORGANIZATION REPORT NUMBER L-17795	
9. SPONSORING/MONITORING AGENCY NAME(S) AND ADDRESS(ES) National Aeronautics and Space Administration Washington, DC 20546-0001			10. SPONSORING/MONITORING AGENCY REPORT NUMBER NASA/TM-1999-209100	
11. SUPPLEMENTARY NOTES				
12a. DISTRIBUTION/AVAILABILITY STATEMENT Unclassified-Unlimited Subject Category 12 Distribution: Standard Availability: NASA CASI (301) 621-0390			12b. DISTRIBUTION CODE	
13. ABSTRACT (Maximum 200 words) The Attitude Control and Energy Storage Experiment is currently under development for the International Space Station; two counter-rotating flywheels will be levitated with magnetic bearings and placed in vacuum housings. The primary objective of the experiment is to store and discharge energy, in combination with existing batteries, into the electrical power system. The secondary objective is to use the flywheels to exert torque on the Station; a simple torque profile has been designed so that the Station's Control Moment Gyroscopes will be assisted in maintaining torque equilibrium attitude. Two energy storage contingencies could result in the inadvertent application of torque by the flywheels to the Station: an emergency shutdown of one flywheel rotor while the other remains spinning, and energy storage with only one rotor instead of the counterrotating pair. Analysis of these two contingencies shows that attitude control and the microgravity environment will not be adversely affected.				
14. SUBJECT TERMS Flywheels, Energy Storage, Attitude Control, Control Moment Gyroscopes, International Space Station			15. NUMBER OF PAGES 20	
			16. PRICE CODE A03	
17. SECURITY CLASSIFICATION OF REPORT Unclassified	18. SECURITY CLASSIFICATION OF THIS PAGE Unclassified	19. SECURITY CLASSIFICATION OF ABSTRACT Unclassified	20. LIMITATION OF ABSTRACT	